Solar Energy Materials & Solar Cells 105 (2012) 46–52

Contents lists available at SciVerse ScienceDirect

Solar Energy Materials & Solar Cells

journal homepage: www.elsevier.com/locate/solmat

Control of CVD-deposited ZnO films properties through water/DEZ ratio: Decoupling of electrode morphology and electrical characteristics

S. Nicolay*, M. Benkhaira, L. Ding, J. Escarre, G. Bugnon, F. Meillaud, C. Ballif

Ecole Polytechnique Fédérale de Lausanne (EPFL), Institute of Microengineering (IMT), Photovoltaics and thin-film electronics laboratory, EPFL-STI-IMT-NE, Rue Breguet 2, CH-2000 Neuchâtel, Switzerland

ARTICLE INFO

Article history:
Received 3 February 2012
Received in revised form
10 May 2012
Accepted 11 May 2012

Keywords:
TCO
ZnO
CVD
Thin film silicon

ABSTRACT

In this work, it is shown that variations in the ratio of oxygen to zinc precursors at constant temperature allow changing the surface morphology of zinc oxide (ZnO) films deposited by low-pressure metalorganic chemical vapor deposition, while keeping the sheet resistance and transparency of the layers constant. This allows developing ZnO layers combining interesting properties such as low surface roughness (below 15 nm) and low sheet resistance (below 15 Ω/□). More generally, it is shown that the pyramidal feature density can be controlled by tuning the precursor flows. This leads to film surfaces characterized by zones with a rough morphology mixed with zones with almost flat features. Therefore, by using this technique, the light-scattering ability of a film can be carefully tuned through its surface morphology without affecting the conductivity or transparency of the layer. This provides an efficient tool to optimize the front electrode of thin-film silicon solar cells to achieve the best possible combination of open-circuit voltage, fill factor and photo-generated current. The presented solution is an in-situ process achievable in standard deposition conditions making it easily up-scalable with existing production equipment.

1. Introduction

In the past decade, interest in zinc oxide (ZnO) has grown in the fields of optoelectronics, active-glass coatings and photovoltaics (PV), fueled by the potential applications of this high-bandgap, high-exciton-binding-energy compound [1]. Regarding thin-film (TF) PV applications, ZnO is the compound of choice to achieve low-cost, reproducible electrode layers on large-scale production lines. ZnO is indeed a transparent conductive oxide (TCO) that has promising advantages compared to the traditionally used indium tin oxide (ITO), whose toxicity, scarcity and price warrant the search for suitable alternatives. This need for an ITO alternative is reinforced as the projected installed capacity of PV modules increases every day [2]. For these reasons, ZnO is nowadays one of the most used TCO materials for TF silicon solar cell development.

Several techniques are available for the deposition of ZnO, among which the most common are metalorganic chemical vapor deposition (MOCVD) [3,4], sputtering [5], molecular beam epitaxy [6] and sol–gel methods [7]. However, for large-scale production purposes, one of the preferred deposition techniques is low-pressure MOCVD (LP-MOCVD). Indeed, ZnO layers produced with this technique, under given growth conditions, are polycrystalline films constituted of large grains with a pronounced preferential orientation (PO) along the $\vec{a}$ axis [8]. This leads to natural staircase-faced pyramids at the surface of the film, which gives LP-MOCVD-grown ZnO strong light-scattering abilities, a prerequisite for TF solar cell applications. In fact, due to the relatively small values of the amorphous and microcrystalline silicon (a-Si:H and μc-Si:H) absorption coefficients, the optical path of the light inside the active layers of Si PV cells has to be increased to enhance the photo-generated current. One possible solution to achieve this goal is to use nano-textured TCO surfaces [9]. In contrast to LP-MOCVD layers, sputtered ZnO films require one additional wet etching process step to achieve a rough light-scattering surface [5]. In addition, achieving sufficiently low sheet resistance ($<20\ \Omega/\square$) necessitates micrometer-thick ZnO layers, which leads to large surface features, imposing a link between the surface morphology and the electrical conductivity of LP-MOCVD ZnO. As-grown LP-MOCVD ZnO presents V-shaped valleys separating the pyramidal features, which causes defective μc-Si growth, leading to decreased open-circuit voltage (V_{oc}) and fill factor (FF), and hence to lower cell efficiency [10]. One possible approach to circumvent these issues is to use a surface plasma treatment to transform the V-shaped valleys into smoother U-shaped valleys that are well-adapted for good-quality absorber material deposition [11]. However, such plasma treatment leads to a decrease in the scattering ability of the film. Besides, it

* Corresponding author. Tel.: +41 32 718 3311; fax: +41 32 718 3201.
E-mail address: sylvain.nicolay@epfl.ch (S. Nicolay).

0927-0248/$ - see front matter © 2012 Elsevier B.V. All rights reserved.
http://dx.doi.org/10.1016/j.solmat.2012.05.016

requires an additional vacuum processing step and is, therefore, not well-suited to production. Another solution would be to decouple the light trapping and electrical properties of the electrodes. This can be achieved by properly designing a master structure with surface features characterized by high scattering ability and a morphology well-suited for Si deposition. Nano-imprint technology can then be used to transfer this master to a large-scale transparent lacquer in combination with a highly conductive material (such as In_2O_3:H) [12]. However, it is not clear yet if any purposefully designed structures will provide better solar cell performance than state-of-the-art as-grown LP-MOCVD ZnO on a scale suitable for production. In addition, the use of In_2O_3:H might be an hindrance to large-area PV module production.

Based on these considerations and in order to foster large-scale future development of TF Si PV, a suitable alternative has to be found. In this paper, we will demonstrate that by carefully tuning the growth parameters of LP-MOCVD ZnO, specifically by changing the precursor flow ratio, it is possible to control the surface morphology while keeping good light-scattering properties, transparency and conductivity. This allows growing conductive films with tuned roughness, thereby relaxing the traditional trade-off between surface morphology and electrical conductivity inherent to LP-MOCVD ZnO films. In combination with high-transparency/conductivity films recently developed by Ding et al., this will strengthen the place of LP-MOCVD ZnO as the material of choice to be used in various TCO-demanding devices such as PV modules [13]. Indeed, both the approaches developed in the following paper and in Ref. 13 (the use of a doping multilayer growth scheme) could be combined in a single deposition process to achieve highly transparent, conductive films with an intentionally controlled surface roughness. It will be demonstrated that the use of these newly developed deposition regimes allows decreasing the defect density in single-junction μc-Si cells from 1.3 to 0 defect/μm. This defect density variation correlates with V_{oc} and FF, which change from 490 to 540 mV and from 59 to 75%, respectively.

2. Experimental

ZnO films were deposited by LP-MOCVD on 4 cm^2 0.5 mm-thick AF45 Schott glass substrates. Diethylzinc (DEZ) and water (H_2O) vapor were used as precursors, and their flows were changed in order to investigate the effects on film properties. Diborane (B_2H_6) diluted at 1% in argon was used as the doping gas, and its flow was adapted to achieve similar free-carrier concentrations in all films. The total pressure was 0.63 mbar (~0.5 Torr) inside the reactor and the growth temperature was 155 °C. The samples were characterized with atomic force microscopy (AFM) and scanning electron microscopy (SEM) to study the surface morphology, while X-ray diffraction (XRD) was used to determine the crystallographic orientations present at different growth stages. The optical properties of the films were measured with a dual-beam UV–vis–NIR Perkin Elmer spectrophotometer (Lambda 900) equipped with an integrating sphere. Absorption spectra were deduced from the transmittance and reflectance spectra measured in air (using diiodomethane (CH_2I_2) as an index-matching liquid to eliminate surface roughness effects). An Ecopia Hall effect measurement setup (HMS5000) was used to determine the sheet resistance and charge carrier sheet density, in the Van der Pauw configuration, at room temperature. From these two values, the Hall mobility (μ_H), charge carrier density (N_H) and resistivity (ρ_H) were calculated. Cell performance (V_{oc}, FF) was characterized in standard conditions with current–voltage (I–V) measurements using an AM 1.5 Wacom sun simulator, while short-circuit current density (J_{sc}) was evaluated through external quantum efficiency measurements between 370 and 1100 nm.

3. Results

Previous studies have shown that growth parameters such as deposition temperature and precursor flows can strongly influence the properties of LP-MOCVD ZnO films [8]. By changing the temperature, the surface morphology was changed from smooth (low temperature) to very rough (high temperature) [8]. However, these changes were concomitant with an increase of the layer sheet resistance, making the films unsuitable for PV applications. Indeed, in the case of low-temperature deposition, the growth occurred by successive re-nucleation of very thin and small grains, leading to a high density of grain boundaries (GBs), while at high temperature, the film exhibited small voids in between large hexagonal grains. As both GBs and voids are obstacles that reduce the mobility of free electrons, changing the deposition temperature resulted in a sharp increase of the film resistivity. In the present work, pressure and deposition temperature were kept constant at the standard process values. The water flow was kept at 20 sccm, while the DEZ flow was varied from 22 to ~4 sccm, so that the water/DEZ ratio changed from ~0.9 to 5. In addition, in order to keep the carrier concentration in the range of 6–8 $\times 10^{19}$ cm^{-3}, the B2H6 flow was also varied between 2.5 sccm (with the lowest DEZ flow) and 5 sccm (for the highest DEZ flow). The electrical properties measured on the different samples are shown in Table 1. Regarding the presented gas flows, it is important to note that the used mass flow controllers were calibrated with N2, as it is usually the case. A gas correction factor should then be applied to calculate actual volume flows. However, this correction factor is not known for gases such as DEZ in the process conditions. Therefore we used the pressure rate of rise technique to estimate the specific actual gas flow in our deposition system from which the precursor ratios were derived. The thickness of the film was kept around 2 μm (+/−150 nm). This allows investigating the effect of the precursor flows on the surface morphology and the resulting optical properties of the films, without modification of free-carrier absorption.

Fig. 1 shows the surface morphology variations observed with AFM as a function of increasing water/DEZ ratio.

Table 1
Electrical properties of the films as a function of the water/DEZ ratio.

Estimated water flow (sccm)	Estimated DEZ flow (sccm)	Estimated B2H6 flow (sccm)	water/DEZ ratio	N_H (cm^{-3})	μ_H (cm^2/Vs)	Sheet resistance (Ohm/□)
20	22	5	0.9	6.50E+19	25	19
20	17.5	5	1.15	7.00E+19	34	13
20	16.5	5	1.2	6.50E+19	35	14
20	15	5	1.3	6.00E+19	36	14
20	11	4.5	1.8	8.00E+19	32	12
20	3.7	2.5	5.2	1.20E+20	3	87

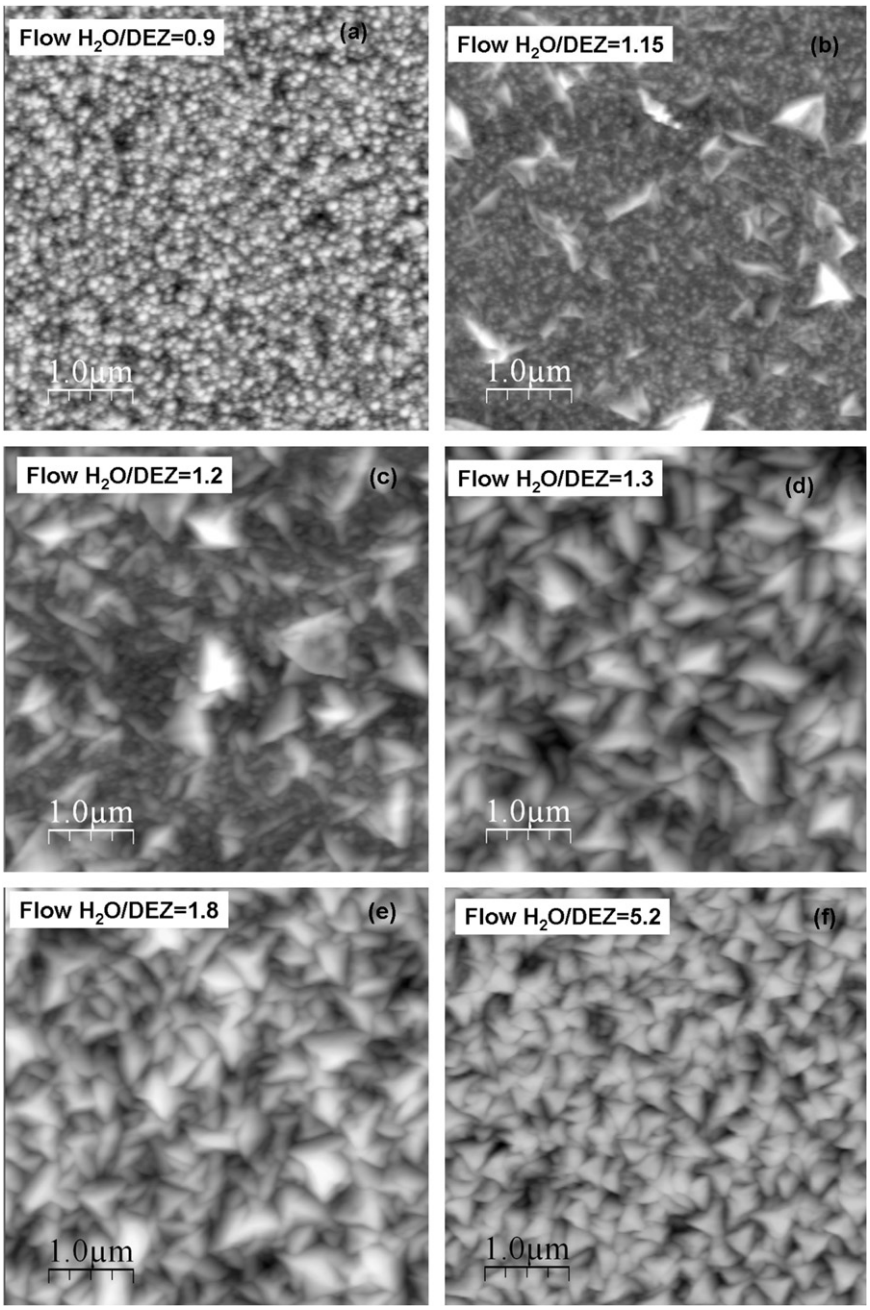

Fig. 1. AFM images showing surface morphology changes as a function of increasing water/DEZ ratio.

Changes in the precursor ratio strongly affect the surface morphology of the films. At the lowest water/DEZ ratio (Fig. 1a), the surface is made of small grains with a few larger "pyramidal" grains emerging. As the ratio is increased, the pyramidal grains become bigger and appear more often on the surface (Fig. 1b). As the ratio is further increased, these pyramidal grains take over the smaller features, and above a ratio of 1.3 (Fig. 1d), the smaller grains cannot be observed anymore. As the ratio is further increased, the shape of the pyramidal grains evolves from large irregularly defined pyramids to smaller more regular-shaped three-sided pyramids (Fig. 1f). The root mean square (RMS) roughness of the different films increases from 15 nm to 30 nm, 45 nm and 70 nm for ratios from 0.9 to 1.3, and then it decreases to 60 nm and 40 nm for ratios of 1.8 and 5.2, respectively. Note that the morphology observed at low water/DEZ ratios is typical of LP-MOCVD ZnO deposited at low temperature. However, in the case of low-temperature deposition, the sheet resistance of the film strongly increases, while in the present case, as will be explained later, it stays below 20 Ω/□.

To characterize pyramid density, an informatics routine using the AFM image data was developed to count the number of surface feature tips having a height above a certain threshold relative to the lowest point measured in the AFM image (a tip being defined as a point with its eight neighboring pixels having a lower height). The results of these calculations are shown in Fig. 2.

As expected, at a low water/DEZ ratio, there are few features with a height above 150 nm. However, the number of peaks above 150 nm increases steeply with the precursor ratio which correlates well with the increase in pyramidal feature density. It is also seen that for layers deposited with a water/DEZ ratio of 1.3 or larger, the number of features above 75 nm and 150 nm is the

same, which indicates that the pyramids are the dominant shapes on the surface of these films. On the contrary, for a ratio of 1.2, only half of the peaks above 75 nm are also above 150 nm indicating in this case that the surface is almost equally divided between large pyramids and smaller features.

Regarding crystallographic orientation variation, it was shown before that the evolution of surface morphology can be closely related to a change in the layer PO [8]. In the present case, the evolution of film PO as a function of the different precursor ratios is shown in Fig. 3a, while Fig. 3b displays the variation of the (0 0 2) and (1 1 0) XRD peak intensities as a function of the water/DEZ ratio. Note that the smaller peaks present between the (1 0 1) and (1 1 0) features are measurement artifacts (arising from the copper radiation used to acquire the spectra).

It is observed that the PO indeed strongly depends on the water/DEZ ratio. For the lowest water/DEZ ratio, the PO is (0 0 2) as is expected from the smoother surface morphology [8]. As the ratio is increased, the (1 1 0) XRD intensity grows and finally dominates for water/DEZ ratios over 1.8. In addition the (1 0 0) peak also becomes more marked with the increase of the water/DEZ ratio. Note that the two small features observed at low ratio on each side of the (1 0 0) peak are measurement artifacts. The gradual change in PO from (0 0 2) $\vec{c}$ axis perpendicular to the substrate to (1 1 0) $\vec{c}$ axis parallel to the substrate is associated with a shift from columnar growth, as observed in sputtered ZnO, toward V-shaped grain growth characteristic of "standard" LP-MOCVD ZnO deposition.[8] As will be explained later in more detail, the observed morphological and crystallographic variations are ascribed to flow-controlled growth competition between the different orientations present in the film at the beginning of the growth.

Since the surface morphology changes, it is expected that the optical behavior of the films will also be modified. This is confirmed in Fig. 4 which displays the haze (diffuse transmittance/total transmittance) measured at a wavelength of 600 nm as a function of water/DEZ ratio.

It can be seen that with the smooth surface features achieved at low water/DEZ ratios, the haze factor is as low as 0% (no light diffusion). As the water/DEZ ratio is increased and as the pyramid density on the surface of the films increases, the haze increases gradually. It reaches a maximum of 35% for a ratio of 1.3, at which the film surface exhibits the largest pyramids, before decreasing as the pyramids become smaller but more regular and sharper. For larger water/DEZ ratios (between 2 and 5, the largest investigated in our case), the haze remains constant around 10%. Eventually, it is also interesting to note that as the estimated DEZ flow is further reduced (below ~12.5 sccm corresponding to a water/DEZ ratio above ~1.5), the film deposition starts to be limited by gas transport to the substrate and not surface kinetics,

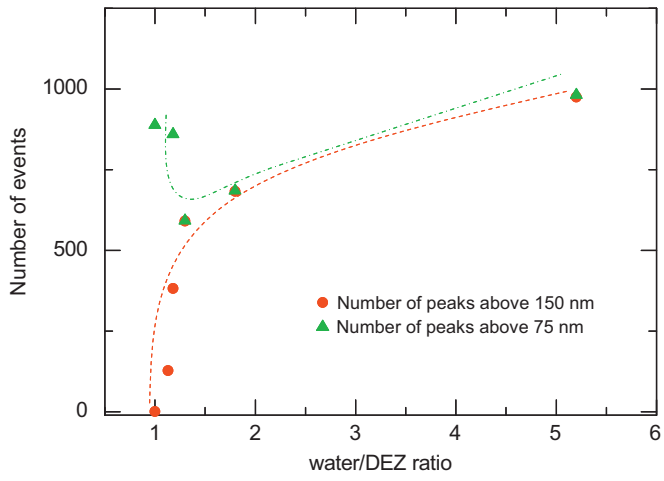

Fig. 2. Variation of peak density as a function of the water/DEZ ratio. (The lines are guides for the eyes).

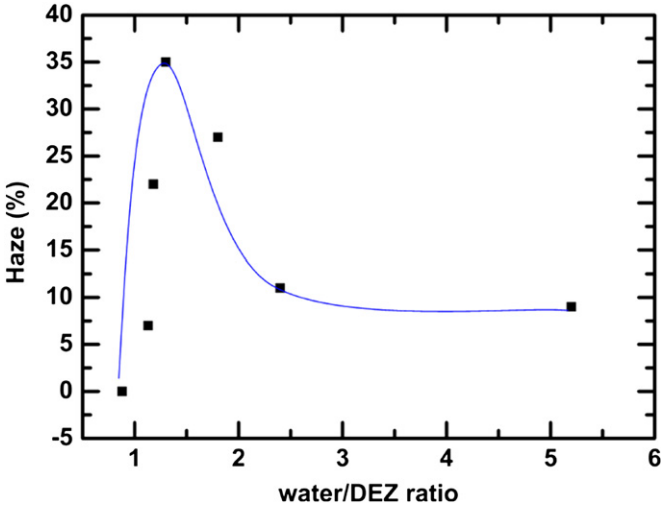

Fig. 4. Haze variation measured at 600 nm as a function of water/DEZ ratio. (The line is a guide for the eyes).

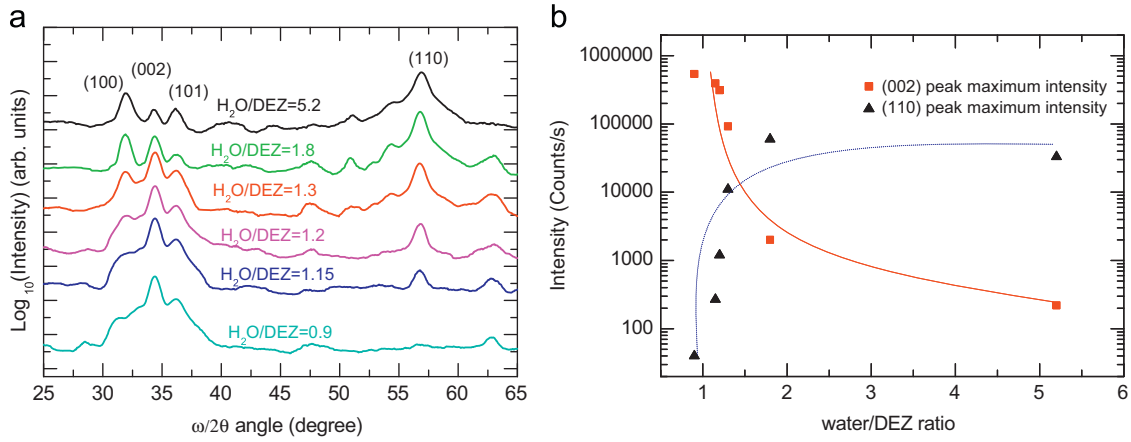

Fig. 3. (a) XRD spectra of films with different water/DEZ ratios. (b) Variation in the intensity of the (0 0 2) and (1 1 0) XRD peaks as a function of the water/DEZ ratio. (The lines are guides for the eyes).

as shown in Fig. 5 where the growth rate dependency on the DEZ flow is plotted.

Regarding the electrical properties of the deposited layers, and as explained in the introduction, the B_2H_6 flow was optimized for each layer in order to achieve a sheet resistance between 10 and 20 Ω/□ and a free-carrier concentration between 6 and 8×10^{19} cm^{-3}. As shown in Table 1, this was possible for all the films but the one with the highest water/DEZ ratio, which was characterized by an unusually low electron mobility of 3 cm^2 V^{-1} s^{-1} and a carrier concentration of 1.2×10^{20} cm^{-3} which led to a measured sheet resistance of 87 Ω/□. One possible explanation for such low mobility could be the higher density of GBs associated to the smaller grain size characteristic of film deposited at the highest water/DEZ ratio (see Fig. 1f). However, in the case of the layer deposited with the lowest ratio, narrow grains (see Fig. 1a) should have also led to low mobility, which was not the case. Therefore, it is suspected that it is the presence of micro-voids in the layer that contribute to the lower free-carrier mobility (this will be further explained in the discussion part and in Fig. 7b). In addition, it has to be noted that the GBs themselves are not oriented in the same crystallographic direction in the films deposited with the lowest and highest water/DEZ ratios. Indeed, for the lowest ratio, they are oriented perpendicular to the $\vec{c}$ axis, while for the highest ratio, they are oriented perpendicular to the (1 1 0) orientation. This might also lead to a difference in GB impact on the free-electron mobility. Eventually, it is interesting to note that as explained in Section 3, a surface morphology similar to the one observed in Fig. 1a has also been observed in a previous work by depositing at low temperature [8]. Nevertheless, in the latter case, low growth temperature deposition also led to a strong increase in the sheet resistance of the film. The difference in electrical properties between these two films characterized by similar surface morphology and crystallographic orientation is attributed to the fact that at low temperature the film grows through a successive re-nucleation phenomenon [8]. This leads to the formation of a layer with a high GB density. On the contrary, we propose that the use of high DEZ flow at standard temperature leads to the formation of continuous columnar growth with lower GB density, ensuring better electron mobility and allowing the combination of a smooth surface morphology and low sheet resistance.

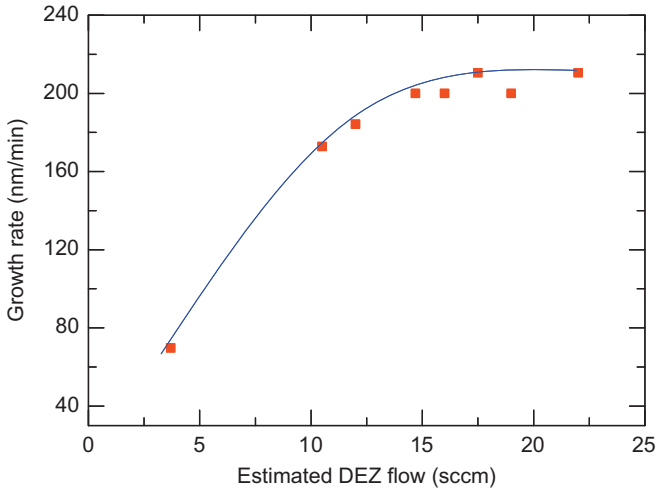

Fig. 5. Growth rate as a function of DEZ flow. (The line is a guide for the eyes).

Based on these promising results, a similar series of TCO samples was deposited to investigate the effect of ZnO surface morphology on defect creation during μc-Si:H growth. 1 μm thick μc-Si:H p-i-n cells were then deposited on the different front electrodes, and the *I–V* characteristics and external quantum efficiencies of the cells were measured. The results are shown in Fig. 6a and b, respectively. As expected, for the lowest water/DEZ ratio, which provides the smoothest morphology, the FF and V_{oc} are the highest while the J_{sc} is the lowest. When the roughness of the front electrode surface increases with the water/DEZ ratio, the FF and V_{oc} decrease due to a higher defect density in the absorber material. However, the rougher substrate provides better light scattering (as seen in Fig. 6a), leading to higher J_{sc}. For water/DEZ ratios higher than 1.5, J_{sc} starts to decrease as well, which is attributed to the formation of the smaller more regular-shaped three-sided pyramids (see Fig. 1f). Despite the reduced RMS roughness of these high water/DEZ ratio morphologies, it is believed that the surface features are sharper leading to higher defect density and therefore to lower FF and V_{oc} values [14].

In order to confirm these suppositions, cross-sectional SEM was performed on the different cells in order to quantify the number of defects in the absorber material (Fig. 7a). Note that defect density counting in the μc-Si:H material was performed with picture brightness and contrast parameters set to the same values for each cross-sectional SEM image. However, regarding the image shown in Fig. 7b, the contrast and brightness were

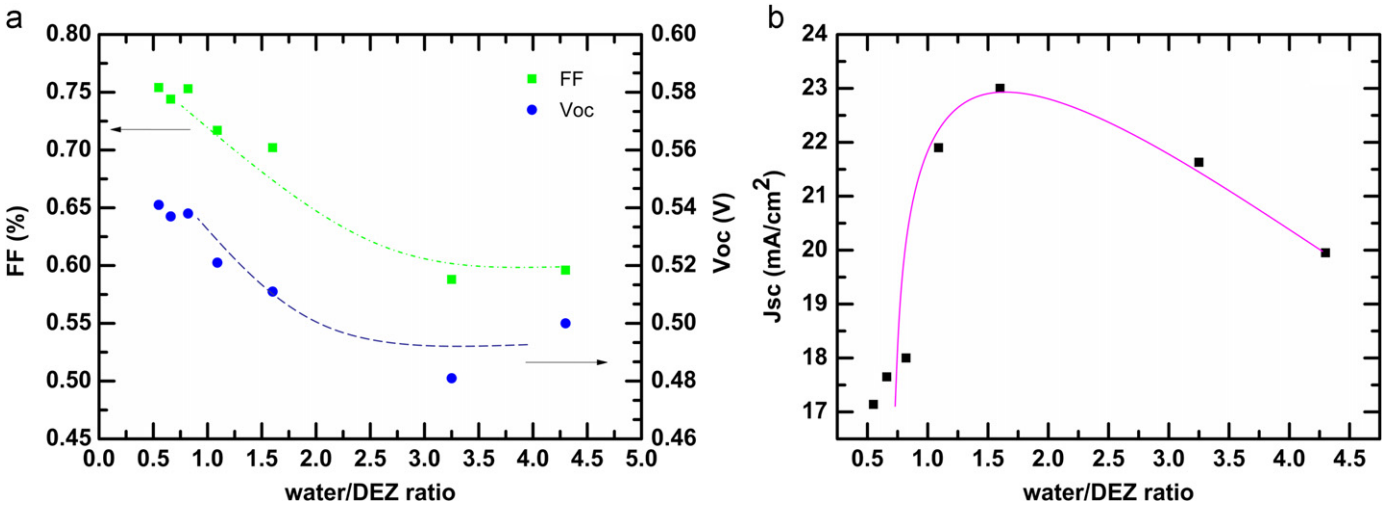

Fig. 6. (a) FF and V_{oc} of 1-μm-thick μc-Si:H cells deposited on different ZnO front electrodes with increasing water/DEZ ratios. (b) J_{sc} calculated from external quantum efficiencies measured on the cells deposited on the different front electrodes. (The lines are guides for the eyes).

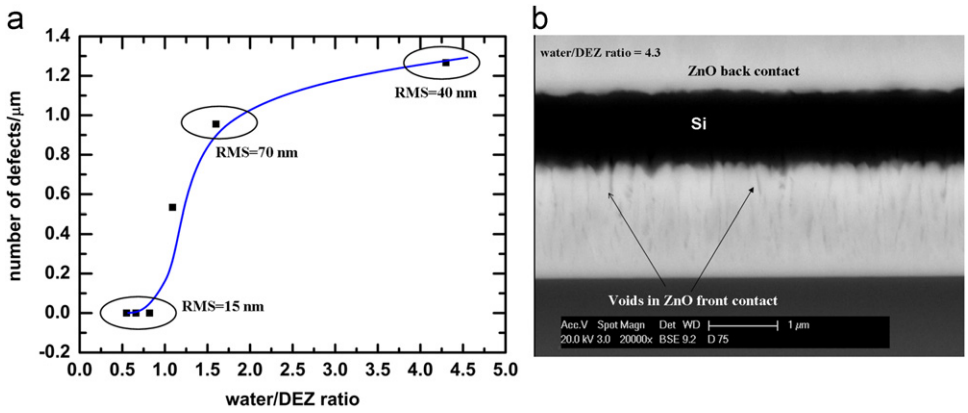

Fig. 7. (a) Defect density as a function of water/DEZ ratio. (The line is a guide for the eyes.) (b) Cross-sectional SEM image with contrast and brightness set to show the ZnO film bulk structure.

tuned to better reveal the bulk structure of the ZnO substrate deposited at high water/DEZ ratio.

Fig. 7a shows that the lowest defect density is indeed observed in the cell deposited on the smoothest substrate, while the highest defect density in μc-Si:H is not observed on the roughest substrate but rather on the highest water/DEZ-ratio electrode, characterized by the sharper features. In this case, voids also clearly appear in the ZnO film (see Fig. 7b). As mentioned before, it is believed that these voids are responsible for the higher sheet resistance (87 Ω/□, see Table 1) of these films.

4. Discussion

Despite the fact that the effects of precursor flow ratio on the surface properties of polycrystalline ZnO have already been investigated, both for LP-MOCVD [15] and for sputtering [16], no clear explanation of how the gas flows impact morphology has been provided up to now. In order to fill this gap, we base our understanding on previous work showing that the morphology observed at the surface of LP-MOCVD ZnO results from a combination of both nucleation- and kinetic-driven phenomena [8–17]. In fact, it was demonstrated that temperature induced inter-facet diffusion could lead to the selection of different crystallographic PO [8]. Indeed, inter-facet diffusion refers to the ability of an incoming adatom to diffuse from one facet (with a low dangling bond density) of an existing cluster to another facet (with a higher dangling bond density) [18]. Hence, the decrease in the adatom inter-facet diffusion limits the vertical growth of the non-minimum surface energy (NMSE) plane (e.g. (1 1 0) or (1 0 0) surfaces with higher dangling bond density) compared to the minimum surface energy (MSE) planes (e.g. (0 0 2) surfaces with lower dangling bond density). As a consequence, grain growth competition between nuclei having NMSE and MSE planes parallel to the substrate surface is hampered. Similarly, we propose here that, for a given water flow, increasing the DEZ flow leads to an increase of the nucleation rate (number of stable nuclei per unit area and time) and to a reduction of the inter-facet diffusion through a diminution of the adatom surface mobility [18,19]. In consequence, this results in the (0 0 2) PO, which is most present in the nucleation stage, remaining the dominant orientation throughout the deposition. This leads to a surface characterized by small hexagonal-tipped features typical of the wurtzite ZnO structure grown along the $\vec{c}$ axis. As the flow of DEZ is decreased, the nucleation density decreases and the surface adatom mobility increases. This fosters inter-facet diffusion promoting competition between nuclei with NMSE planes parallel to the substrate and nuclei with the traditional low surface energy (0 0 2) plane parallel to the substrate. As previously demonstrated, a result of this kinetic-growth competition is a shift from one PO to another, with associated surface morphology modifications.[8] For the films deposited with the lowest DEZ flow, based on growth rate measurements shown in Fig. 5, it is supposed that the process is now taking place in the transport-limited regime. In this case, the authors suggest that the lower amount of precursor atoms arriving on the substrate surface could results in a lower surface coverage. This in turn would yield a lower nucleation rate leading to the formation of a less-dense film made of more-regular grains separated by micro-voids as shown in Fig. 7b.

5. Conclusion

In conclusion, we have demonstrated in this paper that by carefully tuning the precursor ratios, it is possible to control the pyramidal feature density and the feature shape at the surface of LP-MOCVD ZnO films, while keeping low sheet resistance. This allows the decoupling of the surface morphology and light-scattering ability from the electrical properties of the film. The observed changes in film surface morphologies have been ascribed to different precursor flow induced growth competitions between nuclei presenting different crystallographic orientations. It is thus now possible to control the degree of roughness of as-grown LP-MOCVD ZnO layers, without an additional treatment step It was shown that, by controlling the large-surface-feature density, the electrical performance of μc-Si:H cells can be optimized thanks to the reduction of defective zones in the absorber layer. This is similar to what was achieved previously by using a plasma post-treatment to modify the surface. As a consequence, these results open new possibilities to combine good cell electrical properties and large haze factor at the industrial scale. In addition, the possibility to deposit smooth conductive films by LP-MOCVD opens new prospects for this process to be used for LED or OLED electrodes.

Acknowledgment

This work was supported by the EU FP7 Project PEPPER no. 249782 and by the Swiss Federal Office for Energy (OFEN).

References

[1] D.M. Bagnall, Y.F. Chen, Z. Zhu, T. Yao, S. Koyama, M.Y. Shen, T. Goto, Optically pumped lasing of ZnO at room temperature, Applied Physics Letters 70 (1997) 2230–2232.

[2] S. Faÿ, L. Feitknecht, R. Schluchter, U. Kroll, E. Vallat-Sauvain, A. Shah, Rough ZnO layers by LP-CVD process and their effect in improving performances of amorphous and microcrystalline silicon solar cells, Solar Energy Materials and Solar Cells 90 (2006) 2960–2967.
[3] S. Faÿ, J. Steinhauser, S. Nicolay, C. Ballif, Polycrystalline ZnO: B grown by LPCVD as TCO for thin film silicon solar cells, Thin Solid Films 518 (2009) 2961–2966.
[4] A. Hongsingthong, I.A. Yunaz, S. Miyajima M. Konagai, Zno films prepared by two-step MOCVD process for use as front TCO in silicon-based thin film solar cells, in: Proceedings of the 35th IEEE Photovoltaic Specialists Conference, 2010, p. 1508–1511.
[5] O. Kluth, G. Schöpe, J. Hüpkes, C. Agashe, J. Müller, B. Rech, Thin Solid Films, Modified Thornton model for magnetron sputtered zinc oxide: film structure and etching behaviour 442 (2003) 80–85.
[6] Y. Chen, H.-J. Ko, S.-K. Hong, Y. Segawa, T. Yao, Morphology evolution of ZnO (0001) surface during plasma-assisted molecular-beam epitaxy, Applied Physics Letters 80 (2002) 1358–1360.
[7] M. Ohyama, H. Kozuka, T. Yoko, Sol–gel preparation of transparent and conductive aluminum-doped zinc oxide films with highly preferential crystal orientation, Journal of the American Ceramic Society 81 (1998) 1622–1632.
[8] S. Nicolay, S. Faÿ, C. Ballif, Growth model of MOCVD polycrystalline ZnO, Crystal Growth & Design 9 (2009) 4957–4962.
[9] J. Meier, U. Kroll, S. Dubail, S. Golay, S. Faÿ, J. Dubail, A. Shah, Efficiency enhancement of amorphous silicon p-i-n solar cells by LP-CVD ZnO, in: Proceedings of the 28th IEEE Photovoltaic Specialists Conference, 2000, p. 746–749.
[10] M. Python, O. Madani, D. Dominé, F. Meillaud, E. Vallat-Sauvain, C. Ballif, Influence of the substrate geometrical parameters on microcrystalline silicon growth for thin-film solar cells, Solar Energy Materials and Solar Cells 93 (2009) 1714–1720.
[11] J. Bailat, D. Domine, R. Schluchter, J. Steinhauser, S. Faÿ, F. Freitas, C. Bucher, L. Feitknecht, X. Niquille, T. Tscharner, A. Shah C. Ballif, High-efficiency p-i-n microcrystalline and micromorph thin film silicon solar cells deposited on LPCVD ZnO coated glass substrates, in: Proceedings of the IEEE 4th World Conference on Photovoltaic Energy Conversion, vols 1–2, 2006 pp. 1533–1536.
[12] K. Soderstrom, J. Escarre, O. Cubero, F.-J. Haug, S. Perregaux, C. Ballif, UV–nano-imprint lithography technique for the replication of back reflectors for n-i-p thin film silicon solar cells, Progress in Photovoltaics 19 (2011) 202–210.
[13] L. Ding, M. Boccard, G. Bugnon, M. Benkhaira, S. Nicolay, M. Despeisse, C. Ballif, Highly transparent ZnO bilayers by LP-MOCVD as front electrodes for thin-film micromorph silicon solar cells, Solar Energy Materials and Solar Cells 98 (2012) 331–336.
[14] H. Li, R.H. Franken, J.K. Rath, R.E.I. Schropp, Structural defects caused by a rough substrate and their influence on the performance of hydrogenated nano-crystalline silicon n–i–p solar cells, Solar Energy Materials and Solar Cells 93 (2009) 338–349.
[15] M.L. Addonizio, A. Merola, A. Antonaia M. Della Noce, Low pressure-chemical vapour deposition of ZnO thin films: relation between deposition parameters and light scattering properties, in: Proceedings of the 21st EU Photovoltaic Solar Energy Conference, 2006, p. 1.
[16] N. Fujimura, T. Nishihara, S. Goto, J. Xu, T. Ito, Control of preferred orientation for ZnO_x films: control of self-texture, Journal of Crystal Growth 130 (1993) 269–279.
[17] A. Van Der Drift, Evolutionary selection, a principle governing growth orientation in vapour-deposited layers, Philips Research Reports 22 (1967) 267–288.
[18] Y. Kajikawa, S. Noda, H. Komiyama, Comprehensive perspective on the mechanism of preferred orientation in reactive-sputter-deposited nitrides, Journal of Vacuum Science and Technology A21 (2003) 1943–1954.
[19] M. Ohring, Materials Science of Thin Film, 2nd ed., Academic, New York, 2002, p. 383.